Evaluation of Human Immunodeficiency Virus Type 1 Reverse Transcriptase Primer tRNA Binding by Fluorescence Spectroscopy: Specificity and Comparison to Primer/Template Binding

Sara H. Thrall,* Jochen Reinstein, Birgitta M. Wöhrl, and Roger S. Goody*

Max-Planck-Institut für Molekulare Physiologie, Abteilung Physikalische Biochemie, Postfach 102664, 44026 Dortmund, Germany

Received November 6, 1995; Revised Manuscript Received February 5, 1996[⊗]

ABSTRACT: A host cell-derived $tRNA_3^{Lys}$ molecule is utilized by human immunodeficiency virus type 1 (HIV-1) reverse transcriptase (RT) to prime DNA synthesis from the viral RNA genome. We performed fluorescence titration experiments to characterize the interaction between RT and its natural primer, $tRNA_3^{Lys}$, and to address RT's putative role in the required and specific packaging of $tRNA_3^{Lys}$ into the budding virus. Titration of RT with $tRNA_3^{Lys}$ resulted in a 30% maximal quenching of RT tryptophan fluorescence, from which a dissociation constant (K_d) of 57.6 ± 7.5 nM was derived. Titration of RT with *Escherichia coli* $tRNA_2^{Glu}$, *E. coli* $tRNA_2^{Tyr}$, *E. coli* $tRNA^{Lys}$, yeast $tRNA^{Phe}$, or *in vitro*-synthesized human $tRNA_3^{Lys}$ (no base modifications) resulted in similar fluorescence changes and K_d values as obtained for the natural $tRNA_3^{Lys}$. The specific interaction between RT and $tRNA_3^{Lys}$ during viral assembly suggested by previous *in vivo* studies is therefore not present in the fully processed, *in vitro* form of RT. Other factors during viral assembly must therefore cooperate in the packaging of $tRNA_3^{Lys}$. The nonspecific and ionic strength dependent RT−tRNA interaction detected in the present studies suggests that the overall shape and charges of tRNA constitute recognition features for RT binding. The fluorescence of the wyebutine base contained on the anticodon loop of yeast $tRNA^{Phe}$ was found to increase upon RT binding, supporting speculation that RT interacts with the anticodon loop of tRNA. The individual tRNAs also displaced a fluorescent DNA primer/template (p/t) substrate from RT, indicating overlapping tRNA and p/t binding sites. Cubic fit evaluation of the displacement titrations allowed further assessment of the affinities of the two competing ligands. The presence of both overlapping and separate p/t and tRNA binding regions on RT was tested by examination of the affinity of a possible RT bisubstrate type inhibitor, containing motifs proposed to be essential for both tRNA and p/t binding. Reverse transcriptase was found to bind to the mutant tRNA 10-fold more tightly than to the unaltered tRNA (K_d = 4.5 ± 1.0 and 44.6 ± 6.6 nM, respectively). Further analyses revealed that the tighter affinity is probably due to a preferred p/t binding mode and not to one expected if separate tRNA and p/t binding regions are accessed simultaneously by the same molecule.

During assembly of viral proteins of the human immunodeficiency virus type 1 (HIV-1),[1] the three isoacceptors of $tRNA^{Lys}$ are selectively packaged into the newly budding virions, from a pool of over 150 different tRNAs present in the cell (Jiang *et al.*, 1993; Söll, 1993). Replication of the viral RNA genome (vRNA) is then initiated from the 3′ end of one of these specifically packaged $tRNA^{Lys}$ isoforms, $tRNA_3^{Lys}$ [for review, see Marquet *et al.* (1995)]. Eighteen nucleotides of the $tRNA_3^{Lys}$ become annealed to the complementary primer binding site (PBS) on the vRNA, thereby forming the transcription initiation complex from which reverse transcriptase (RT) catalyzes proviral DNA synthesis (LeGrice, 1993; Litvak *et al.*, 1994). Understanding the components involved in the packaging and binding of the primer $tRNA_3^{Lys}$ and how it is directed to the PBS to form the initiation complex may lead to the identification of promising targets for the design of effective drugs against HIV proliferation.

Participation of RT in the specific sequestering of primer $tRNA_3^{Lys}$ from the infected cell during viral assembly has been suggested, most convincingly by *in vivo* studies carried out by Kleiman and co-workers (Mak *et al.*, 1994). These authors transfected COS-7 cells with various HIV proviral DNA constructs and quantitated the tRNA molecules incorporated into the virus produced. They showed that, while $tRNA^{Lys}$ makes up approximately 6% of the total tRNAs in the cell, 60% of the tRNAs found in virions were $tRNA^{Lys}$, of which 40% were isoacceptor form 3. This selectivity was lost, however, when the cells were transfected with a mutant proviral DNA lacking 95% of the RT gene. Transfer RNA^{Lys} was specifically incorporated even when the proviral DNA lacked a primer binding site sequence, suggesting that the complementarity between the PBS and 18 nucleotides of the $tRNA_3^{Lys}$ molecule is not responsible for its specific uptake. Since RT is still part of a larger precursor protein ($Pr160^{gag\text{-}pol}$)

* To whom correspondence should be addressed. Telephone: (49) 231/1206-380. Fax: (49) 231/1206-229. E-mail: roger.goody@mpi-dortmund.mpg.de.

⊗ Abstract published in *Advance ACS Abstracts,* March 15, 1996.

[1] Abbreviations: HIV-1, human immunodeficiency virus type 1; K_d, dissociation constant; PBS, primer binding site; PCR, polymerase chain reaction; RT, reverse transcriptase; natural $tRNA_3^{Lys}$, transfer ribonucleic acid, isoacceptor 3, *in vivo* form, contains base modifications; synthetic $tRNA_3^{Lys}$, transfer ribonucleic acid, isoacceptor 3, T7 RNA polymerase *in vitro* synthesized, contains no base modifications; vRNA, viral RNA genome.

0006-2960/96/0435-4609$12.00/0

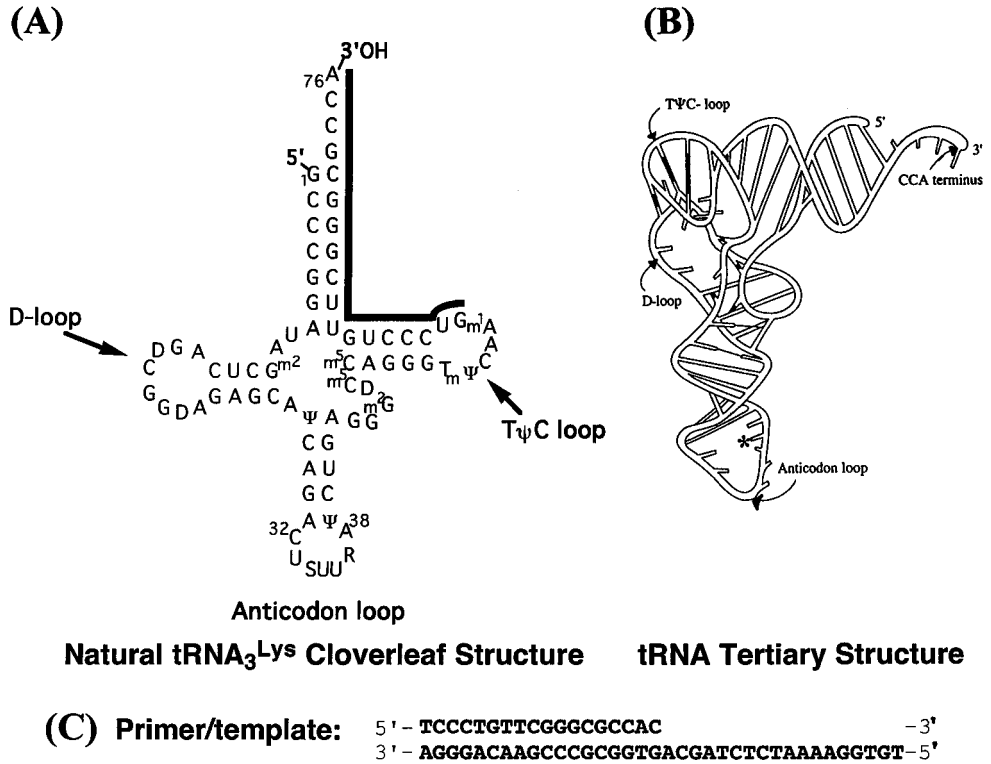

FIGURE 1: Structures of natural $tRNA_3^{Lys}$ and duplex DNA primer/template used in these studies. (A) Cloverleaf structure of $tRNA_3^{Lys}$, depicting sequence, modified bases, D, TψC, and anticodon loops, and location of the 18 nucleotides of the 3′ end (marked with a bold line) which become annealed to the viral RNA for initiation of transcription. (B) Tertiary, L-shaped structure inherent to tRNA molecules. Stacking of the acceptor and TψC stems forms a continuous, A-form double helical region, of about 11 bases in length. Tertiary interactions between the TψC and D loops result in the 90° bend in the molecule and formation of the second arm containing the anticodon loop. The asterisk marks the position of the fluorescent wyebutine (Y) base at position 37 on yeast $tRNA^{Phe}$ [adapted from Abeles *et al.* (1992)]. (C) Sequence of the 36/18-mer duplex DNA primer/template molecule used in the titrations.

when $tRNA_3^{Lys}$ is carried into the newly budding virions, the *in vivo* studies did not determine whether the RT portion alone confers the selective $tRNA^{Lys}$ binding.

In its *in vitro*, and presumably *in vivo*, fully processed form, RT exists as a heterodimeric enzyme, composed of an asymmetric arrangement of a 66 kDa (p66) subunit, containing the polymerase and RNaseH active sites, and a 51 kDa (p51) subunit, derived from proteolytic truncation of the larger subunit (LeGrice, 1993). The *in vitro* interaction between $tRNA_3^{Lys}$ and RT has been detected in several labs by gel-shift assay (Barat *et al.*, 1989, 1993; Richter-Cook *et al.*, 1992; Oude-Essink *et al.*, 1995), footprinting (Sarih-Cottin *et al.*, 1992; Wöhrl *et al.*, 1993), and cross-linking studies (Barat *et al.*, 1989; Mishima & Steitz, 1995). Taken together, these studies suggested that both the p51 and p66 subunits of RT interact with tRNA and that several portions of the tRNA molecule, including the anticodon loop and the D and TψC loops, as well as the acceptor stem of the tRNA (see Figure 1) interact with RT. But while Barat *et al.* (1989) reported a specific interaction between $tRNA_3^{Lys}$ and RT, other groups showed that RT can interact in a similar manner with different tRNAs, as well as utilize different tRNAs to prime reverse transcription (Kohlstaedt & Steitz, 1992; Weiss *et al.*, 1992b; Sobol *et al.*, 1991). Any specific interaction with RT was suggested to involve the anticodon loop of $tRNA_3^{Lys}$ (Barat *et al.*, 1989; Sarih-Cottin *et al.*, 1992). Nonetheless, the *in vivo* work demonstrated that a mutant $tRNA_3^{Lys}$ in which the anticodon was changed from UUU to CUA was packaged into the virus as effectively as the wild-type $tRNA_3^{Lys}$ (Huang *et al.*, 1994). To date, no detailed and quantitative investigations of tRNA binding by RT have been made to resolve these apparent discrepancies.

Previously, RT tryptophan fluorescence and fluorescently labeled substrates were used to characterize the binding of a DNA/DNA primer/template duplex (p/t) and nucleotides (Müller *et al.*, 1991b; Divita *et al.*, 1993; Rittinger *et al.*, 1995). Here we show that the intrinsic fluorescence of RT can also be used as a signal for the interaction between RT and tRNA. We evaluated the affinity and specificity of $tRNA_3^{Lys}$ binding to RT and compared these results to those of p/t binding. The affinities obtained by RT tryptophan titrations were confirmed by extrinsic fluorescence titrations, using the naturally fluorescent base in the anticodon loop of yeast $tRNA^{Phe}$, and by titrations of tRNA displacing a fluorescently labeled primer/template from RT. We also describe the use of a cubic fit analysis of displacement titrations as a viable method for evaluation of the binding of two competing ligands. The extent of overlapping tRNA and p/t binding sites was next addressed by measurement of the affinity of a possible bisubstrate type RT inhibitor, designed to contain both tRNA- and p/t-like features. The methodology employed in this work will allow examination of possible factors contributing to the specific uptake of $tRNA_3^{Lys}$ into virus, the mechanism of tRNA binding and annealing to the vRNA PBS, as well as provide a convenient method for evaluation of possible inhibitors to these processes.

MATERIALS AND METHODS

Proteins. Recombinant HIV reverse transcriptase was expressed in *Escherichia coli* and purified as described before (Müller *et al.*, 1989, 1991a). Highly homogeneous prepara-

tions of the heterodimeric form of the enzyme were used, resulting from coexpression of the 66 and 51 kDa subunits. Enzyme concentrations were routinely determined by using an extinction coeffecient of 260 450 M^{-1} and by Bradford analysis (Bradford, 1976), using a gravimetrically prepared solution of RT as standard.

Cloning of the 5′ Overhang Mutant $tRNA_3^{Lys}$ Gene. The cloning of the plasmid for T7 *in vitro* transcription synthesis of the 5′ overhang mutant $tRNA_3^{Lys}$ (shown in figure 5) was carried out by standard recombinant PCR techniques, similar to those used for the cloning of the $tRNA_3^{Lys}$ gene (Clackson *et al*., 1991; Weiss *et al.*, 1992a). Briefly, PCR amplification of the $tRNA_3^{Lys}$ gene contained on the plasmid ptRNA,Lys3 (Weiss *et al.*, 1992b) was carried out by using one primer which inserts an *Eco*RI restriction site, a T7 promoter sequence, and nine additional bases onto the tRNA gene (5′-AATAAGAATTCTAATACGACTCACTATAGGGAATGG-CGCCCGGATAGCTCAGTC-3′) and another primer containing sequences complementary to 12 bases of the 3′ end of the $tRNA_3^{Lys}$ gene, and which inserts *Bam*HI and *Nsi*I restriction sites (5′-AATAAGGATCCATGCATGGCGC-CCGAAC-3′). PCR was carried out according to manufacturer's instruction (Hybaid OmniGene, MWG-Biotech). The 129-base pair PCR product, containing the 5′-extended $tRNA_3^{Lys}$ gene and a T7 promoter and flanked by *Bam*HI and *Eco*RI restriction sites, was digested with *Eco*RI and *Bam*HI and ligated into pUCBM21 (Boehringer Mannheim) between the *Eco*RI and *Bam*HI sites. The resulting plasmid (2828 bp), called pBMT7OHLys, was transformed into *E. coli* XL1 cells and its sequence confirmed by standard sequencing methods. The plasmid pBMT7OHLys was used for the synthesis of the 5′ overhang mutant $tRNA_3^{Lys}$, lacking modified bases, from the T7 promoter (see below).

tRNAs. Pure bovine $tRNA_3^{Lys}$, which has the same sequence and base modifications as human $tRNA_3^{Lys}$ (Isel *et al.*, 1993), was a gift from Stefan Weiss [see Weiss *et al.* (1992b) for purification and analysis]. *E. coli* $tRNA_2^{Glu}$, *E. coli* $tRNA_2^{Tyr}$, *E. coli* $tRNA^{Lys}$, and yeast $tRNA^{Phe}$ were purchased from Sigma. All tRNAs were gel-purified, if required, and renatured, as described below. Synthetic human $tRNA_3^{Lys}$ and 5′ overhang $tRNA_3^{Lys}$ were prepared by T7 RNA polymerase *in vitro* transcription of the plasmids pBMT7Lys or pBMT7OHLys, respectively (see below).

In Vitro Transcriptions. $tRNA_3^{Lys}$ was synthesized by T7 RNA polymerase *in vitro* transcription of a DNA fragment obtained by PCR amplification of the human $tRNA_3^{Lys}$ gene contained on the plasmid pBMT7Lys (Weiss *et al.*, 1992a,b). PCR was carried out by using the following primers: 5′-TGGCGCCCGAACAGGGACTTG-3′ and 5′-ACGCCA-GGGTTTTCCCAGTCACG-3′. The resulting 143 bp DNA fragment (approximately 300 ng), containing the $tRNA_3^{Lys}$ gene and the T7 promoter, was directly used in the *in vitro* transcription reaction (see below). The 5′ overhang mutant tRNA was synthesized by *in vitro* transcription (see below) of a DNA template generated by restriction endonuclease cleavage of the plasmid pBMT7OHLys containing the mutant tRNA gene and the T7 promoter (described above). The plasmid (10 μg) was restriction digested with *Nsi*I and *Nde*I (New England Biolabs), and the 5′ end of the tRNA gene, created by the *Nsi*I cleavage, was blunt-ended by treatment with the Klenow fragment (Promega), according to the manufacturer's protocol. The resulting DNA fragments (2513 and 315 bp) were purified through a NucTrap column (Stratagene) to remove excess deoxynucleotides. *In vitro* transcription of the 315 bp fragment containing the mutant tRNA gene and the T7 promoter was carried out without removal of the rest of the plasmid DNA (2513 bp fragment). *In vitro* transcriptions were carried out by use of the T7-MEGAshortscript kit, according to the manufacturer's protocol (Ambion).

tRNA Purification and Analysis. The 76-base $tRNA_3^{Lys}$ or 85-base 5′ overhang $tRNA_3^{Lys}$ *in vitro* transcripts, as well as all other impure tRNAs, were purified by electrophoresis through a 10% acrylamide/8 M urea denaturing gel. The tRNA band was viewed by UV shadowing (Sambrook *et al*., 1989), excised from the gel, and eluted by the RNaid Kit (BIO 101), according to the manufacturer's protocols. The size and purity of tRNAs were checked by denaturing polyacrylamide gel electrophoresis followed by ethidium bromide staining or by autoradiography of denaturing gels of [^{32}P]tRNAs 5′ end-labeled by treatment with [γ-^{32}P]ATP and T4 polynucleotide kinase, according to standard protocols (Sambrook *et al*., 1989). Before use, all tRNAs were heated to 80 °C, for 10 min, in buffer containing 25 mM NaCl, 0.2 mM $MgCl_2$, and 10 mM Tris-HCl (pH 7.5), and then cooled slowly to room temperature. The renatured tRNAs were rechecked before and after use by denaturing gel electrophoresis to ensure that no degradation occurred during the heating or the experiment. Transfer RNA concentrations were determined spectrophotometrically, using appropriate molecular weights and assuming an absorbance of 1.0 at 260 nm equals 37 μg of RNA. The secondary structural elements of the synthetic $tRNA_3^{Lys}$ and of the mutant overhang $tRNA_3^{Lys}$ (shown in Figure 5) were predicted by the RNA secondary structure prediction program RNAfold in PC/Gene, based on the Zuker method (Jacobson *et al.*, 1984).

Oligodeoxynucleotides and Primer/Template Formation. The 36-mer and 18-mer oligodeoxynucleotides (for sequences, see Figure 1) oligodeoxynucleotides were synthesized on an Applied Biosystems 380 B DNA synthesizer and purified by standard procedures. The oligodeoxynucleotides were annealed by heating an equimolar mixture of both in 50 mM NaCl and 20 mM Tris-HCl (pH 7.5) for 10 min at 70 °C, followed by cooling to room temperature over a period of ca. 2 h in a water bath.

Preparation of Fluorescence-Labeled Primer/Template. The 18/36 primer/template was labeled with a fluorescent thymidine derivative [succinylfluorescein-labeled ddTTP (SFddTTP), DuPont-New England Nuclear] at the 3′ end of the primer, as described earlier (Müller *et al.*, 1991a,b). The concentration of the resulting labeled 19/36-mer was determined by degradation with exonuclease III (Boehringer Mannheim), followed by comparison of the resulting fluorescence intensity with that of the free labeled nucleoside triphosphate at known concentrations.

Fluorescence Titrations. Fluorescence titrations were performed using an SLM Smart 8100 spectrofluorometer equipped with a PH-PC 9635 photomultiplier. The buffer contained 50 mM Tris-HCl (pH 8.0), 10 mM $MgCl_2$, 50 or 5 mM KCl (as indicated), and 1 mM dithiothreitol in a total volume of 0.7 mL. For tryptophan fluorescence, the samples were excited at 295 nm and the emission intensity was measured at 340 nm (slit widths of 1 and 16 nm, respectively). All data were corrected for the background intensity of the buffer, for dilution, and for the inner filter effect. Measurements were made in a 0.5 cm path length cuvette

to minimize the filter effect, and the residual effect was estimated in control experiments using *N*-acetyltryptophanamide and increasing concentrations of the oligonucleotide. Data were transferred to a personal computer and evaluated using the commercially available fitting program Grafit (Erithacus Software). A quadratic equation analogous to the one given by Müller *et al.* (1991b) describing the binding equilibrium was used for the fitting procedure. Values for the dissociation constant (K_d), the amplitude of the fluorescence change, and the enzyme concentration were allowed to vary during the fit procedure. For experiments with fluorescent primer/template, excitation was at 500 nm and the emission intensity was measured at 532 nm (slit widths set at 2 and 8 nm for excitation and emission, respectively). The affinities of tRNAs and nonfluorescent p/t derived by displacement of fluorescent p/t were determined by fitting the data to a cubic equation (see below). For titrations with the fluorescent yeast $tRNA^{Phe}$, excitation was at 335 nm, and emission intensity was measured at 443 nm (slit widths set at 2 and 16 nm for excitation and emission, respectively). The contribution to the emission intensity at wavelength 443 nm by RT at high concentrations was subtracted from the data. All experiments were done at a temperature of 25 °C.

Data Analysis of Fluorescence p/t Displacement Titrations. The dissociation constants of tRNAs and p/t were determined in competition experiments with labeled p/t and made use of the known K_d of the labeled p/t determined in a direct titration with RT (as described above). The general mathematical description of this system is the solution of a cubic equation. This solution is not based on any assumptions with respect to the relationship of the total concentrations of the participating ligands to the respective dissociation constants. This complete analysis is specifically required if the affinities of the two ligands are very high such that the corresponding K_d values are much lower than the initial concentration of the substance to be titrated.

A kinetic system where the ligands B and C compete for binding to A is described in Scheme 1, where in this case A corresponds to RT and B and C correspond to the fluorescent primer/template and tRNA or nonfluorescent primer/template.

Scheme 1

$$A + B \underset{K_{d_{AB}}}{\rightleftharpoons} AB \quad A + C \underset{K_{d_{AC}}}{\rightleftharpoons} AC$$

The dissociation constants $K_{d_{AB}}$ and $K_{d_{AC}}$ are defined as follows:

$$K_{d_{AB}} = \frac{[A_f][B_f]}{[AB]}; \quad K_{d_{AC}} = \frac{[A_f][C_f]}{[AC]} \tag{1}$$

$[A_f]$, $[B_f]$, and $[C_f]$ are the free concentrations of A, B, and C, respectively; $[A_o]$, $[B_o]$, and $[C_o]$ are the corresponding total concentrations and [AB] and [AC] the concentrations of the complexes. If the concentrations of B and C are much higher than that of A, then the observed dissociation constant of the AC complex, $K_{d_{AC(obs)}}$, is defined by the simple relationship

$$K_{d_{AC(obs)}} = K_{d_{AC}}\left(1 + \frac{[B_f]}{K_{d_{AB}}}\right) \approx K_{d_{AC}}\left(1 + \frac{[B_o]}{K_{d_{AB}}}\right) \tag{2}$$

If the concentrations of B and C are close to that of A, however, the assumption that $[C_f] \cong [C_o]$ and $[B_f] \cong [B_o]$ no longer holds. The deviation from a simple hyperbolic binding is most evident if $[A_o] >> K_{d_{AB}}$ and $K_{d_{AC}}$. The general solution of the system in Scheme 1 is the solution of a cubic equation. This solution is not based on any assumptions with respect to the relationship of $[A_o]$, $[B_o]$, and $[C_o]$ to $K_{d_{AB}}$ and $K_{d_{AC}}$. Equation 1 may be solved for [AB] with the use of the mass equations $[A_o] = [A_f] + [AB] + [AC]$, $[B_o] = [B_f] + [AB]$, and $[C_o] = [C_f] + [AC]$ to give $[AC]^3 + a_1[AC]^2 + a_2[AC] + a_3 = 0$ with the following coefficients:

$$a_0 = K_{d_{AB}} - K_{d_{AC}} \tag{3}$$

$$a_1 = ([A_o](K_{d_{AC}} - K_{d_{AB}}) + [B_o](2K_{d_{AC}} - K_{d_{AB}}) + [C_o]K_{d_{AB}} - {K_{d_{AB}}}^2 + K_{d_{AB}}K_{d_{AC}})/a_0 \tag{4}$$

$$a_2 = ([A_o][B_o](K_{d_{AB}} - 2K_{d_{AC}}) - [B_o]^2K_{d_{AC}} - [B_o]K_{d_{AB}}([C_o] + K_{d_{AC}}))/a_0 \tag{5}$$

$$a_3 = \frac{[A_o][B_o]^2K_{d_{AC}}}{a_0} \tag{6}$$

The general solution of a cubic equation is obtained as described (Press *et al.*, 1989):

$$Q \equiv \frac{{a_1}^2 - 3a_2}{9}; \quad R \equiv \frac{2{a_1}^3 - 9a_1a_2 + 27a_3}{54} \tag{7}$$

If $Q^3 - R^2 \geq 0$, there are three solutions of the cubic equation:

$$\Theta = \arccos\left(\frac{R}{\sqrt{Q^3}}\right) \tag{8}$$

$$[AB]_1 = -2\sqrt{Q}\cos\left(\frac{\Theta}{3}\right) - \frac{a_1}{3} \tag{9}$$

$$[AB]_2 = -2\sqrt{Q}\cos\left(\frac{\Theta + 2\pi}{3}\right) - \frac{a_1}{3} \tag{10}$$

$$[AB]_3 = -2\sqrt{Q}\cos\left(\frac{\Theta + 4\pi}{3}\right) - \frac{a_1}{3} \tag{11}$$

However, only one out of the three solutions given above is meaningful and has to be selected automatically by an appropriate algorithm.

In the rare case where $R^2 - Q^3 > 0$, there is only one solution:

$$[AB] = -\text{sign}(R)\left[(\sqrt{R^2 - Q^3} + |R|)^{1/3} + \frac{Q}{(\sqrt{R^2 - Q^3} + |R|)^{1/3}}\right] - \frac{a_1}{3} \tag{12}$$

The equations above were included in a program written in Turbo Pascal that minimizes the deviations of measured and

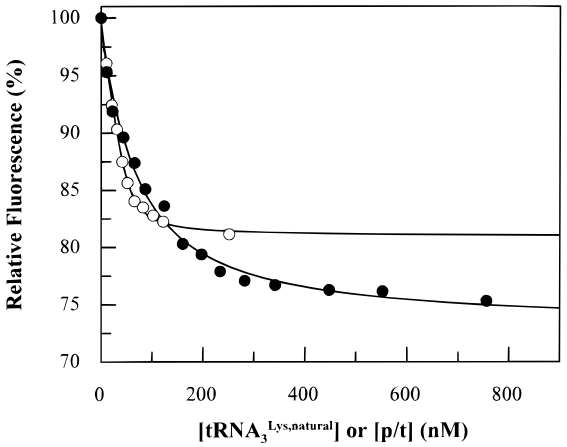

FIGURE 2: Titration at 25 °C of HIV-1 RT (40 nM) with its natural primer for initiation of transcription, $tRNA_3^{Lys}$ (●), or with the 18/36-mer primer/template (○) (see Figure 1) using tryptophan fluorescence as a signal of binding. The protein fluorescence (λ_{ex} = 295 nM, λ_{em} = 340 nM) was monitored in a 700 μL solution containing 40 nM RT, 10 mM $MgCl_2$, 50 mM KCl, 1 mM DTE, and 50 mM Tris-HCl (pH 8.0). The curves show the best fit of the data to the quadratic equation describing the binding of the tRNA or primer/template to a single site in the heterodimeric form of the enzyme. The fits gave K_d values of 57.6 ± 7.5 nM for the $tRNA_3^{Lys}$−RT interaction (and a 30% maximal quenching of fluorescence) and 5.7 ± 0.9 nM for the p/t−RT interaction (and a 23% maximal quenching of fluorescence).

calculated data points by a nonlinear Nelder−Mead least square optimization algorithm (Press *et al*., 1989).

RESULTS AND DISCUSSION

Titration of RT Fluorescence with $tRNA_3^{Lys}$. The HIV-1 reverse transcriptase heterodimer contains 37 tryptophan residues (19 in the p66 subunit and 18 in the p51 subunit). Previous work in our laboratory described the tryptophan fluorescence quenching of RT upon binding of a duplex DNA primer/template (18/36-mer), or a poly(rA)/$(dT)_{15}$ template/primer, from which dissociation constants and binding rates were derived (K_d values of ca. 1.8−7 nM; Divita *et al.*, 1993; Rittinger *et al.*, 1995). As shown in Figure 2, the tryptophan fluorescence of RT is also quenched upon the addition of $tRNA_3^{Lys}$. Fitting of the data in Figure 2 by nonlinear regression to a quadratic equation describing the binding equilibrium (see Materials and Methods) resulted in a value of 57.6 ± 7.5 nM for the dissociation constant of $tRNA_3^{Lys}$ (compared to 5.7 ± 0.9 nM for p/t binding) and a maximal quenching of fluorescence of 30% (compared to 23% for p/t). Titration of $tRNA_3^{Lys}$ to RT in the same buffer containing 5 mM instead of 50 mM KCl (data not shown) revealed a higher affinity (8.4 ± 1.2 nM at 5 mM KCl compared to 57.6 ± 7.5 nM at 50 mM KCl; Table 1). The approximately 6-fold increase in affinity for $tRNA_3^{Lys}$ under lower ionic strength conditions suggests that many of the interactions between RT and $tRNA_3^{Lys}$ are electrostatic in nature. A much less dramatic salt effect was seen for p/t binding (3.3 ± 1.5 nM at 5 mM *vs* 5.7 ± 0.9 nM at 50 mM KCl; Table 1).

Evaluation of tRNA Binding Specificity. The groundwork of these studies lies in the assumption that, if RT selects $tRNA_3^{Lys}$ from the infected host cell, it must be able to bind this tRNA more tightly than the other tRNAs also present in the cell. Using the results from the *in vivo* work of Kleiman and co-workers (Mak *et al.*, 1994), the difference

Table 1: Dissociation Constants (K_d) Obtained from Titration of RT Tryptophan Fluorescence with Various tRNAs or with the 18/36 Duplex DNA Primer/Template (p/t)[a]

tRNA	K_d (nM)	
	50 mM KCl	5 mM KCl
natural $tRNA_3^{Lys}$	57.6 ± 7.5	8.4 ± 1.3
synthetic $tRNA_3^{Lys}$	44.6 ± 6.6	21.1 ± 2.8
E. coli $tRNA_2^{Tyr}$	57.5± 4.3	10.3 ± 1.8
E. coli $tRNA^{Lys}$	66.5 ± 4.4	11.2 ± 1.9
yeast $tRNA^{Phe}$	ND	9.8 ± 1.9
E. coli $tRNA_2^{Glu}$	ND	10.2 ± 2.9
p/t (18/36-mer)	5.7 ± 0.9	3.3 ± 1.5

[a] Determined at 25 °C, in buffer containing 50 mM Tris-HCl (pH 8.0), 10 mM $MgCl_2$, 1 mM DTE, and 50 mM or 5 mM KCl, as indicated. Dissociation constants were obtained by fitting the data to the quadratic equation as described in Materials and Methods.

in affinity between $tRNA^{Lys}$ and the other tRNAs in the cell required for the selectivity can be calculated. The ratio of the K_d values for $tRNA^{Lys}$ and all other tRNAs in the cell can be defined as

$$\frac{K_{dB}}{K_{dA}} = \frac{[E\cdot A][B]}{[E\cdot B][A]} \qquad (13)$$

where K_{d_A} is the dissociation constant for the interaction between $tRNA^{Lys}$ and RT (and/or other factors responsible for the specific uptake of $tRNA^{Lys}$), K_{d_B} is the average dissociation constant for the nonspecific interaction with all other tRNAs in the cell, [A] is the concentration of $tRNA^{Lys}$ in the cell, [B] is the concentration of all other tRNAs in the cell, [E·A] is the concentration of RT (and/or other factors) complexed to $tRNA^{Lys}$ during uptake into the virus, and [E·B] is the concentration of RT (and/or other factors) complexed nonspecifically to other tRNAs during uptake into the virus. Assuming that the concentration of all tRNAs in the cell exceeds the concentration of all factors involved in the uptake of $tRNA^{Lys}$ into virions, the percentages of tRNAs found in the cell and in the virus can be substituted into eq 13. $tRNA^{Lys}$ makes up approximately 6% of all tRNAs in the cell (=[A]), meaning other tRNAs in the cell make up ≅94% of tRNAs (=[B]). In the virion, $tRNA^{Lys}$ makes up ≅60% of all tRNAs ([E·A]), where all other tRNAs then make up ≅40% ([E·B]). If RT were solely responsible for the specific uptake of $tRNA^{Lys}$, its affinity for $tRNA^{Lys}$ would therefore have to be more than 23 times greater than the average affinity for the other ≅150 tRNAs in the cell.

An affinity reduced 20-fold compared to that of $tRNA_3^{Lys}$ would be reflected in K_d values in the range of 1 μM for other tRNAs. We therefore carried out RT tryptophan fluorescence titrations to measure the affinities of tRNAs containing significantly different sequences and base modifications, the results of which are summarized in Table 1. All tRNAs tested are shown to bind to RT with affinities similar to those of natural $tRNA_3^{Lys}$ and to display the same ionic strength dependence as was seen for natural $tRNA_3^{Lys}$. Dissociation constants in the range of ca. 60 nM in 50 mM KCl buffer and ca. 10 nM in 5 mM KCl buffer were obtained. In the case of the synthetic form of $tRNA_3^{Lys}$ (containing no base modifications), a slightly reduced affinity in 5 mM KCl (K_d value of ca. 20 nM) was found when compared to those of the other tRNAs. At 50 mM KCl, however, a similar binding affinity was measured for the unmodified $tRNA_3^{Lys}$ compared to the other tRNAs.

These results demonstrate that RT, in its fully processed, p66/p51 heterodimeric form, is unable to discriminate between $tRNA_3^{Lys}$, the tRNA essential to the life cycle of the virus, and other tRNA molecules. Additional components of the viral assembly machinery must therefore play a role in the sequestration of $tRNA_3^{Lys}$ molecules. One suggestion is that RT within the larger $Pr160^{gag\text{-}pol}$ protein is responsible for specific $tRNA^{Lys}$ uptake (Mak *et al.*, 1994). Earlier, the nucleocapsid protein (NC), also part of the unprocessed precursor protein, was postulated to act together with RT to select $tRNA^{Lys}$, since the *in vitro* formation of a ternary complex between tRNA, RT, and NC was detected (Barat *et al.*, 1993). Also important to consider is the fact that in solution, and presumably in the cell, tRNA exists in at least three different conformational states, the distribution of which is shifted by salt concentration, temperature, and aminoacylation (Rigler & Wintermeyer, 1983). It is unknown to what extent the conformation of the $tRNA^{Lys}$ sequestered is also present in the *in vitro* conditions used in the present experiments. Furthermore, complexation of aminoacylated tRNAs in cells to elongation factors is thought to stabilize the conformation of the tRNA required for recognition by the ribosomes (Jamiak *et al.*, 1990). To date, it is also unknown whether $tRNA^{Lys}$ uptake into HIV occurs while the tRNA is complexed to the elongation factor, or to other cellular proteins, nor whether it is aminoacylated during the selection process.

Titration of Yeast $tRNA^{Phe}$ Fluorescence with RT. We also carried out fluorescence measurements wherein an extrinsic signal was used to monitor the tRNA−RT interaction. The fluorescence of the wyebutine (Y) base, located at position 37 in the anticodon loop of yeast $tRNA^{Phe}$ (see Figure 1), has been used extensively to characterize the conformational states of the tRNA (Rigler & Wintermeyer, 1983; Striker *et al.*, 1989; Labuda & Augustyniak, 1977), as well as its interaction with phe-tRNA synthetase (Ehrlich *et al.*, 1980a,b) or with the ribosome A site as part of the phe-$tRNA^{Phe}$/EF-Tu/GTP ternary complex (Rodnina *et al.*, 1993). As shown in Table 1, titration of RT tryptophan fluorescence revealed no significant difference in affinity between yeast $tRNA^{Phe}$ and natural $tRNA_3^{Lys}$ (K_d values of 9.8 and 8.4 nM, respectively). Figure 3 depicts the >30% maximal fluorescence increase of $tRNA^{Phe}$ upon titration with RT in buffer containing 5 mM KCl. The best fit of the data to a quadratic equation (see Materials and Methods) describing the binding of the $tRNA^{Phe}$ to a single site on the enzyme yielded a K_d value of 9.3 ± 2.7 nM that agrees well with that determined from the RT tryptophan fluorescence titration (K_d = 9.8 ± 1.9 nM). Further evaluation of the titration data shows that the stoichiometry of the binding is 1:1 (RT:$tRNA^{Phe}$), in contrast to a 2:1 ratio estimated previously by gel-shift analyses (Richter-Cook *et al.*, 1992). Titration of the Y base fluorescence of $tRNA^{Phe}$ with RT also revealed a lower affinity under higher salt conditions (K_d value of 59.8 ± 15.7 nM in buffer containing 50 mM KCl, data not shown) as was detected by the titrations of RT tryptophan fluorescence.

The enhancement of the Y base fluorescence upon RT binding supports previous indications that the anticodon region interacts with RT (Mishima & Steitz, 1995; Wöhrl *et al.*, 1993). Conversely, the fluorescence increase may be due to a change in conformation of the anticodon in response to interactions of other parts of the tRNA with the enzyme. While footprinting studies reported contact of one side of the anticodon loop of $tRNA_3^{Lys}$ (bases 32−36, see Figure 1) to RT, they also detected a slightly enhanced exposure of the other face of the loop, at base 38, to S1 nuclease cleavage (Wöhrl *et al.*, 1993). The fluorescence change of the Y base at position 37 of $tRNA^{Phe}$ upon RT binding may therefore be detection of the same conformational change of the anticodon loop.

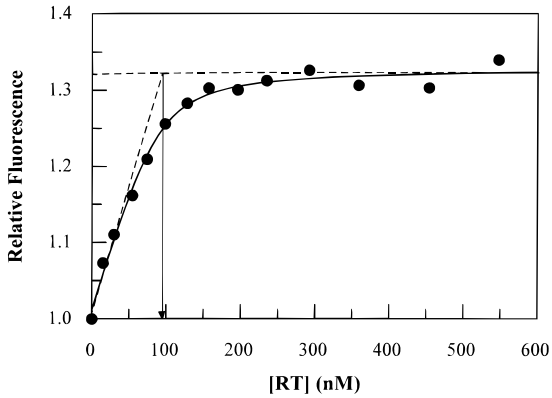

FIGURE 3: Titration at 25 °C of the naturally fluorescent yeast $tRNA^{Phe}$ (90 nM) with RT. RT was titrated into a 700 μL solution containing 10 mM $MgCl_2$, 5 mM KCl, 1 mM DTE, 50 mM Tris-HCl (pH 8.0), and 90 nM $tRNA^{Phe}$. The increase in fluorescence of the $tRNA^{Phe}$ (λ_{ex} = 335 nM, λ_{em} = 433 nM) upon addition of RT was used as a signal of binding (●). The best fit of the data to a quadratic equation yielded a K_d value of 9.3 ± 2.7 nM and a maximal fluorescent enhancement of 33%. The dashed line drawn through the initial data points in the titration represents extrapolation of the data when all RT additions result in a binding event, and the horizontal dashed line represents extrapolation of the data points when saturation of all $tRNA^{Phe}$ molecules by RT has occurred. The arrow drawn from the intersection of these lines indicates the concentration of RT when all $tRNA^{Phe}$ molecules are bound (≅90 nM), corresponding to the approximate stoichiometry of 1:1.

Displacement of Primer/Template by tRNAs. Previous work showed that RT binds a fluorescently labeled DNA/DNA primer/template species with an affinity comparable to that of the unlabeled primer/template (Müller *et al.*, 1991b; Divita *et al.*, 1993; Rittinger *et al.*, 1995). Furthermore, the displacement of the fluorescently labeled p/t was suggested to provide another means for assessment of the affinities of competitive, nonfluororescent p/t species (Müller *et al.*, 1991b). In order to address whether the tRNA and p/t binding sites are overlapping, the ability of tRNA to displace the fluorescent p/t from RT was tested. Figure 4A shows the increase in fluorescence of the labeled p/t upon titration with RT, from which the best fit to the quadratic equation gave a K_d value of 3 nM. Displacement of the labeled p/t into solution from a preformed complex with RT, by the binding of nonfluorescent p/t or of $tRNA_3^{Lys}$ (Figure 4B), results in a decrease in fluorescence intensity of the fluorophore. In order to derive binding constants from the titration data, a cubic equation was used which defines the concentrations of both RT bound and free species at equilibrium, after each p/t or $tRNA_3^{Lys}$ addition (see Materials and Methods). The curves in Figure 4B depict the best fit to the cubic equation when the K_d value of the fluorescent p/t was set to that derived from the direct titration data shown in Figure 4A (3 nM). The K_d values obtained from the fits were 0.6 ± 0.1 nM for the nonfluorescent p/t and 10.9 ± 2.1 nM for natural $tRNA_3^{Lys}$.

The K_d values derived from displacement titrations are within the range expected for p/t and tRNA in the low salt

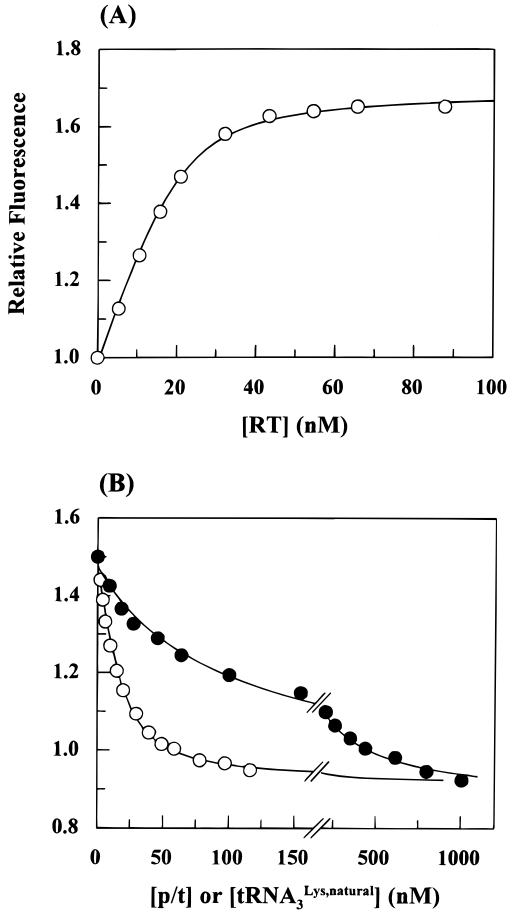

FIGURE 4: RT binding and displacement titrations at 25 °C of a fluorescent primer/template. The 19/36-mer corresponds to the primer/template shown in Figure 1C with an additional fluorescent 3′-dideoxythymidine residue at the 3′ end of the primer (succinylfluorescein -labeled ddTTP). (A) RT was titrated into a 700 μL solution containing 10 mM $MgCl_2$, 5 mM KCl, 1 mM DTE, 50 mM Tris-HCl (pH 8.0), and a constant concentration of the fluorescent primer/template (21 nM). The increase in fluorescence ($\lambda_{ex} = 500$ nM, $\lambda_{em} = 532$ nM) of the primer/template was used as a signal of binding (○) from which the best fit gave a K_d value of 2.97 ± 0.42 nM and a maximal fluorescent enhancement of 69%. (B) A complex between RT (20 nM) and the fluorescent p/t (30 nM) was formed in a 700 μL solution containing 10 mM $MgCl_2$, 5 mM KCl, 1 mM DTE, and 50 mM Tris-HCl (pH 8.0). The solution was then titrated with the unlabeled form of the same p/t (○) or by natural $tRNA_3^{Lys}$ (●). The curves in both titrations show the best fit of the data to the cubic equation (see Materials and Methods) which yielded K_d values of 10.9 ± 2.1 nM for natural $tRNA_3^{Lys}$ and 0.6 ± 0.1 nM for p/t.

buffer (5 mM KCl). The affinity derived for $tRNA_3^{Lys}$ from this displacement titration ($K_d = 10.9 \pm 2.1$ nM) is indistinguishable from that derived from the direct, RT intrinsic fluorescence titration (8.4 ± 1.3 nM; see Table 1). Displacement titrations carried out with other tRNAs gave similar K_d values (Table 2), and all the tRNAs tested completely displaced the fluorescent p/t from RT. Primer/template and tRNA binding are therefore mutually exclusive, indicating that the p/t binding groove, seen in the crystal structure of a duplex DNA p/t complexed to RT, can also accomodate all or portions of the tRNA molecule (Jacobo-Molina *et al.*, 1993).

tRNA vs Primer/Template Binding: Engineering of a Tighter-Binding tRNA Molecule. RT binds its natural primer, $tRNA_3^{Lys}$, with apparently no preference over other tRNA molecules containing significantly different sequences and

Table 2: Dissociation Constants (K_d) Obtained from Displacement of Fluorescently Labeled p/t (30 nM) from RT (20 nM) by Nonfluorescent tRNA or by p/t[a]

tRNA	K_d (nM)
natural $tRNA_3^{Lys}$	11
synthetic $tRNA_3^{Lys}$	15
E. coli $tRNA_2^{Tyr}$	9.3
E. coli $tRNA_2^{Glu}$	12
p/t (18/36-mer)	0.58

[a] A preformed complex between 20 nM RT and 30 nM fluorescently labeled p/t was titrated with nonfluorescent tRNA or p/t (see text for explanation). Titrations were performed at 25 °C, in a solution containing 50 mM Tris-HCl (pH 8.0), 10 mM $MgCl_2$, 1 mM DTE, and 5 mM KCl. Dissociation constants were obtained by fitting the data to the cubic equation as described in Materials and Methods.

base modifications. tRNA recognition by RT may therefore reside in general secondary or tertiary structural elements of the L-shaped tRNA molecule, as opposed to any specific nucleic acid−protein interaction. Displacement of p/t by tRNA suggests that the two molecules share common structural features to be accomodated by similar regions on the protein. The crystal structure of RT complexed to p/t showed that the 18/19-mer duplex DNA assumes an A-form in the first five to seven bases of the duplex, followed by a 40−45° bend in the DNA, as the rest of the duplex assumes a B-form, extending from the polymerase active site into the RNaseH active site (Jacobo-Molina *et al.*, 1993). Since stacking of the acceptor and TψC stems of tRNA also forms an A-form double helix, (Saenger, 1988; see Figure 1B), it is conceivable that this region of tRNA binds to RT in the same vicinity as does the A-form, duplex region of the p/t (e.g. near the polymerase active site). This shared region may be responsible for the displacement of p/t by tRNA.

Nonetheless, it is plausible that certain regions of RT may contribute to p/t binding but not to tRNA binding, and vice versa. Recent work in our lab indicated that the single-stranded, 5′ overhang region of this p/t molecule contributes favorably to its affinity (Rittinger *et al.*, manuscript in preparation). When compared to the affinity of the duplex 18/36 p/t containing an 18-nucleotide, single-stranded 5′ overhang, this work found an affinity reduced 10-fold for both a blunt-ended 19/19 duplex DNA molecule and a 22/22-mer DNA duplex containing four-nucleotide, 3′ overhang ends. In keeping with this, recent enzymatic footprinting and modeling studies of primer/template−RT replication complexes suggested that, in addition to the duplex region of p/t, RT covers up to six or seven nucleotides of the 5′ single-stranded region (Wöhrl *et al.*, 1995). These authors modeled a seven-nucleotide, 5′ overhang onto the 18/19-mer p/t complexed to RT in the crystal structure, which revealed several potentially important interactions between the single-stranded, 5′ region and the p66 fingers subdomain of RT. Since tRNA does not contain a 5′ overhang, these additional interactions with the p66 fingers probably do not occur, which may explain the greater than 10-fold difference in affinities between p/t and tRNA.

The obvious differences between the p/t and tRNA structures also give precedence for the existence of p/t and tRNA specific binding regions on RT, separate from an overlapping region. Specifically, the linear p/t extends by at least 20 bases in length from the polymerase active site into the RNaseH active site, which is an extended structure that presumably cannot be easily adopted by the bulkier

tRNA molecule. Similarly, the putative binding of the double-helical portion of the acceptor stem area of tRNA as well as the anticodon region (suggested by the $tRNA^{Phe}$ Y base titrations in this study and by footprinting and cross-linking studies; Wöhrl *et al.*, 1993; Mishima & Steitz, 1995) means RT would somehow accomodate several structural motifs, separated by a 90° angle, and not present in the linear, duplex p/t. The significance of this recognition by RT of the L shape of tRNA was supported recently by gel-shift assays which found a marked reduction in affinity of RT for tRNAs which were mutated in regions (TψC or D loop) thought to be crucial for stabilization of the L shape (Oude-Essink *et al.*, 1995).

We tested two possible models of tRNA and p/t binding by examining the affinity of a $tRNA_3^{Lys}$ molecule tailored to contain motifs proposed to be important to both p/t binding and tRNA binding. The resulting mutant tRNA, depicted in Figure 5A, contains p/t type binding motifs, an extended duplex region and a 5′ overhang, and tRNA type binding motifs, an L shape consisting of the acceptor stem, the D and T loops, and the anticodon stem and loop.

Two possible binding modes were then considered. In the first, the binding sites of tRNA and p/t are completely overlapping, such that addition of the 5′ overhang on tRNA only adds more favorable interactions, resulting in an increased affinity similar to the 10-fold enhanced affinity seen for a duplex DNA extended by a 5′ overhang. In the second possible scenario, p/t and tRNA binding sites are overlapping but not identical (shared regions that diverge into p/t and tRNA specific subsites). Addition of the p/t motifs onto the tRNA could then have an effect similar to the design of a potent bisubstrate inhibitor, whereby the entropic advantage of simultaneously filling the shared regions and separate subsites of p/t and tRNA binding by the same molecule could result in an affinity in the picomolar or subpicomolar range (Jencks, 1981).

The binding of the overhang $tRNA_3^{Lys}$ to RT, determined by intrinsic fluorescence measurements, is compared to that of the unaltered $tRNA_3^{Lys}$ in Figure 5B. The best fit of the data to the quadradic equation assigned a K_d value of 4.5 ± 1.0 nM to the overhang and 44.6 ± 6.6 nM to the normal tRNA. The affinity of the tRNA was therefore increased by 10-fold upon addition of the p/t motifs, similar to the effect seen upon addition of a 5′ overhang onto a duplex DNA containing blunt ends or 3′ overhangs. Further characterization of the mutant tRNA suggested that it is recognized by RT as a primer/template, since it is also a self-priming substrate for dNTP incorporation onto the 3′ end (data not shown). Furthermore, like duplex DNA p/t binding, the affinity of the overhang was found to be unchanged under lower salt conditions (K_d = 4.9 ± 1.0 nM in buffer containing 5 mM KCl, data not shown).

Addition of the p/t motifs did not result in the dramatic increase in affinity expected if the overlapping as well as separate primer tRNA and duplex p/t binding regions are simultaneously filled by the binding of this mutant tRNA. According to our proposed binding models, this result suggests that the tRNA and p/t binding sites are completely overlapping. Addition of a 5′ overhang region onto a tRNA molecule appears to have only resulted in the formation of more favorable contacts of RT, as was seen for the higher affinity observed for a 5′ overhang duplex DNA compared to one containing blunt ends or a 3′ overhang.

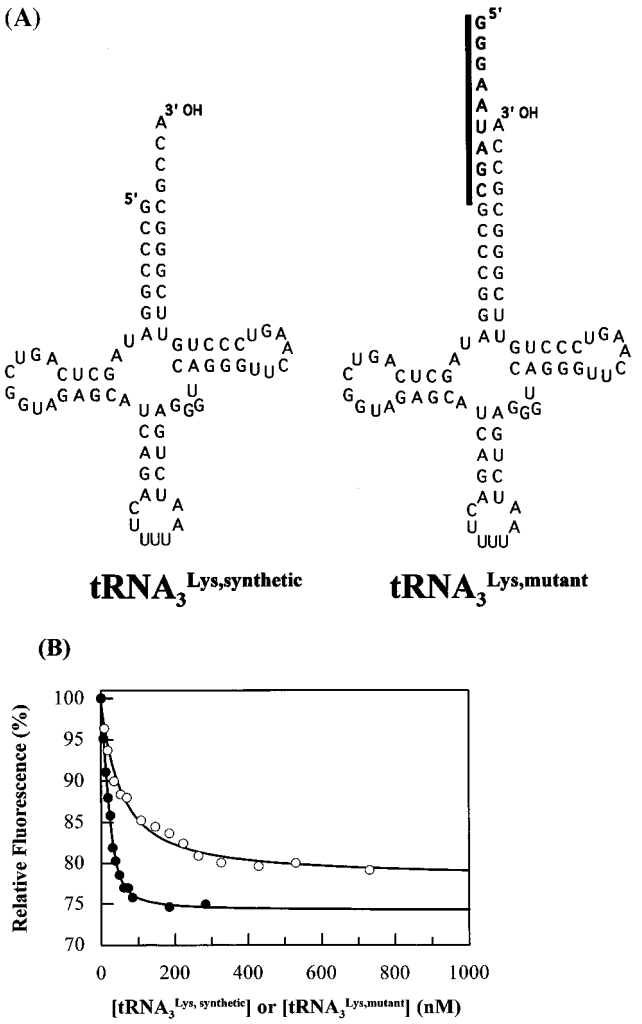

FIGURE 5: Titration at 25 °C of HIV-1 RT (40 nM) tryptophan fluorescence with a synthetic form of $tRNA_3^{Lys}$ (no base modifications) or with a $tRNA_3^{Lys}$ mutant containing p/t- in addition to tRNA-like structural motifs. (A) The cloverleaf structures of synthetic $tRNA_3^{Lys}$ and the 5′ overhang mutant $tRNA_3^{Lys}$. The extra nine bases of the mutant tRNA, adding a 5′ overhang and extended duplex region, are marked with a bold line. (B) The RT tryptophan fluorescence (λ_{ex} = 295 nM, λ_{em} = 340 nM) was monitored after each addition of synthetic $tRNA_3^{Lys}$ (○), or 5′ overhang mutant $tRNA_3^{Lys}$ (●), in a 700 μL solution containing 40 nM RT, 10 mM $MgCl_2$, 50 mM KCl, 1 mM DTE, and 50 mM Tris-HCl (pH 8.0). The curves show the best fit of the data to the quadratic equation which gave K_d values of 44.6 ± 6.6 nM for the $tRNA_3^{Lys}$−RT interaction (20% maximal quenching of fluorescence) and 4.5 ± 1.0 nM for the mutant $tRNA_3^{Lys}$−RT interaction (25% maximal quenching of fluorescence).

Another interpretation that must also be considered is that the addition of the overhang and a longer duplex region in the tRNA repositions the bound molecule such that regions of RT specific to tRNA binding are no longer utilized. Considering the comparable sizes of tRNA and RT [each arm of tRNA is approximately 70 Å long (Saenger, 1988); the p66 subunit of RT has the dimensions of 110 Å by 30 Å by 45 Å (Kohlstaedt *et al.*, 1992)], it is possible that alignment of the 3′ and 5′ ends of the mutant tRNA into the polymerase active site orients the rest of the molecule such that additional tRNA or p/t specific binding regions cannot be accessed. The fact that the maximal fluorescence change (ca. 25%) of the overhang tRNA is greater than was seen for either the unaltered tRNA or p/t (ca. 20% for both) indicates that RT tryptophans are quenched to a greater

extent. Whether this indicates a different binding mode compared to either p/t or tRNA remains to be addressed.

CONCLUSIONS

The specific packaging of $tRNA^{Lys}$ into budding virions must involve the binding by viral components to this tRNA at least 20 times more tightly than to the other tRNAs present in the infected cell. The affinity measurements performed in this work strongly suggest that HIV-1 RT binds its cognate primer, $tRNA_3^{Lys}$, with no discrimination over other tRNAs. A lack of specificity was also found for the interaction between RT from Moloney murine leukemia virus (MoMLV) and its cognate primer, $tRNA^{Pro}$ (Panet & Berliner, 1978). But in contrast to the significant enrichment of $tRNA^{Lys}$ population found in HIV, $tRNA^{Pro}$ is apparently not as selectively packaged into MoMLV, since it was not the most abundant tRNA found in the virus (Harada *et al.*, 1979). A specific interaction, however, was detected *in vitro* between the avian myeloblastosis virus (AMV) RT and its cognate primer, $tRNA^{Trp}$, which was also found to be a highly selected tRNA (30% of the viral tRNA population; Panet *et al.*, 1975; Erickson & Erickson, 1970). Gel-filtration studies showed an apparent selection by AMV RT of this tRNA from a pool of unfractionated cellular or viral tRNAs, which was later reflected in an affinity of $tRNA^{Pro}$ enhanced 2−5-fold over those of other tRNAs (Panet *et al.*, 1975; Hizi *et al.*, 1977). It is unclear whether the tRNA pools used in these studies were free of other cellular or viral components.

Since HIV RT is probably involved in the specific packaging of $tRNA_3^{Lys}$ during viral assembly, our results imply that efforts toward blocking this important early step in HIV replication should focus on the unprocessed form of RT, within the precursor protein

$Pr160^{gag\text{-}pol}$ (Mak *et al.*, 1994). The other members of this unprocessed protein, such as the integrase or gag proteins, may cooperate with the RT portion in a specific interaction with $tRNA_3^{Lys}$. Other cellular components and factors should also be considered, especially in light of the conformational variability of tRNA, and the fact that most tRNAs present in the cell are complexed to other proteins, such as tRNA synthetases and elongation factors (Söll, 1993).

The lack of any specific interaction between $tRNA_3^{Lys}$ and HIV-1 RT as well as the enhanced affinity under lower ionic strength conditions suggest that the general shape and charge of the tRNA constitute the main feature of recognition. Since tRNA can fully displace a duplex DNA p/t from RT, portions of the tRNA molecule can bind to regions of the same cleft involved in p/t binding, as seen in the crystal structure of p/t-complexed RT (Jacobo-Molina *et al.*, 1993). Whether binding of tRNA to RT also induces the dramatic conformational change observed for the binding of p/t (opening by ca. 30 Å of the p66 thumb subdomain, observed by comparison of p/t-complexed and uncomplexed RT crystal structures; Jacobo-Molina *et al.*, 1993; Rodgers *et al.*, 1995) remains to be addressed. Preliminary time-resolved analyses of tRNA binding, however, revealed a multiphasic protein fluorescence decrease, which may correspond to more than one RT conformation during tRNA binding (Thrall *et al.*, manuscript in preparation).

The binding of the 3′ end as well as the anticodon end of the L-shaped tRNA would mean that RT accomodates structural motifs not present in the linear p/t molecule. The presence of a tRNA specific subsite on RT, separate from the p/t binding site, was tested by measurement of the affinity of a mutant tRNA designed to contain both p/t and tRNA structural motifs. The only 10-fold enhanced affinity of the mutant tRNA compared to that of the unaltered tRNA indicates that production of a bisubstrate type ligand, which could result in an increased affinity of several magnitudes, was not achieved. Instead, the additional duplex and 5′ overhang regions on the mutant tRNA appear to have resulted in a preferred p/t binding mode. Unless a tRNA specific region can no longer be accessed by the mutant tRNA, due to size constraints, these results imply that the tRNA and p/t binding sites are completely overlapping. The bulkier shape of the tRNA molecule, as well as the lack of a 5′ overhang, may therefore account for the more than 10-fold weaker binding of the tRNA compared to that of p/t.

The work presented here provides the groundwork for characterization of the mechanism of tRNA binding, the formation of a competent transcription initiation complex, and the examination of possible inhibitors to these processes.

ACKNOWLEDGMENT

We thank Karin Vogel-Bachmayr for her excellent assistance with synthetic $tRNA_3^{Lys}$ preparation and purification and Drs. Katrin Rittinger and Elmar Weinhold for helpful discussions.

REFERENCES

Abeles, R. H., Frey, P. A., & Jencks, W. P. (1992) in *Biochemistry*, pp 271−272, Jones and Bartlett Publishers, Inc., Boston.

Barat, C., Lulien, V., Schatz, O., Keith, G., Nugeyre, M. T., Grüninger-Leitch, F., Barre-Sinoussi, F., LeGrice, S. F. J., & Darlix, J. L. (1989) *EMBO J. 8*, 3279−3285.

Barat, C., LeGrice, S. F. J., & Darlix, J. L. (1991) *Nucleic Acids Res. 19*, 751−757.

Barat, C., Schatz, O., LeGrice, S. F. J., & Darlix, J. L. (1993) *J. Mol. Biol. 231*, 185−190.

Bradford, M. M. (1976) *Anal. Biochem. 72*, 248−254.

Clackson, T., Güssow, D., & Jones, P. T. (1991) in *PCR: A Practical Appproach* (Rickwood, D., & Hames, B. D., Eds.) pp 187−213, Oxford University Press, New York.

Divita, G., Müller, B., Immendörfer, U., Gautel, M., Rittinger, K., Restle, T., & Goody, R. S. (1993) *Biochemistry 32*, 7966−7971.

Ehrlich, R., Lefevre, J. F., & Remy, P. (1980a) *Eur. J. Biochem. 103*, 145−153.

Ehrlich, R., Lefevre, J. F., & Remy, P. (1980b) *Eur. J. Biochem. 103*, 155−159.

Erickson, E., & Erickson, R. L. (1970) *J. Mol. Biol. 52*, 387−390.

Harada, F., Peters, G., & Dahlberg, J. E. (1979) *J. Biol. Chem. 254*, 10979−10985.

Hizi, A., Leis, J. P., & Joklik, W. K. (1977) *J. Biol. Chem. 252*, 6878−6884.

Huang, Y., Mak, J., Cao, Q., Li, Z., Wainberg, M. A., & Kleiman, L. (1994) *J. Virol. 68*, 7676−7683.

Isel, C., Marquet, R., Keith, G., Ehresmann, C., & Ehresmann, B. (1993) *J. Biol. Chem. 268*, 25269−25272.

Jacobo-Molina, A., Ding, J., Nanni, R. G., Clark, A. D., Lu, X., Tantillo, C., Hughes, S. H., & Arnold, E. (1993) *Proc. Natl. Acad. Sci. U.S.A. 90*, 6320−6324.

Jacobson, A. B., Good, L., Simonetti, J., & Zuker, M. (1984) *Nucleic Acids Res. 12*, 45−52.

Jamiak, F., Dell, V. A., Abrahamson, J. K., Watson, B. S., Miller, D. L., & Johnson, A. E. (1990) *Biochemistry 29*, 4268−4277.

Jencks, W. P. (1981) *Proc. Natl. Acad. Sci. U.S.A. 78*, 4046−4050.

Jiang, J., Mak, J., Ladha, A., Cohen, E., Klein, M., Rovinski, B., & Kleiman, L. (1993) *J. Virol. 67*, 3246−3253.

Kohlstaedt, L., & Steitz, T. A. (1992) *Proc. Natl. Acad. Sci. U.S.A. 89*, 9652−9656.

Kohlstaedt, L., Wang, J., Friedman, J. M., Rice, P. A., & Steitz, T. A. (1992) *Science 256*, 1783−1790.
Labuda, D., & Augustyniak, J. (1977) *Eur. J. Biochem. 79*, 303−307.
LeGrice, S. F. J. (1993) in *Reverse Transcriptase* (Skalka, A. M., & Goff, S. P., Eds.) pp 163−191, Cold Spring Harbor Laboratory Press, Cold Spring Harbor, NY.
Litvak, S., Sarih-Cottin, L., Fournier, M., Andreola, M., & Tarrago-Litvak, L. (1994) *Trends Biochem. Sci. 19*, 114−118.
Mak, J., Jiang, M., Wainberg, M. A., Hammarskjöld, M. L., Rekosh, D., & Kleiman, L. (1994) *J. Virol. 68*, 2065−2072.
Marquet, R., Isel, C., Ehresmann, C., & Ehresmann, B. (1995) *Biochimie 77*, 113−124.
Mishima, Y., & Steitz, J. A. (1995) *EMBO J. 14*, 2679−2687.
Müller, B., Restle, T., Weiss, S., Gautel, M., Sczakiel, G., & Goody, R. S. (1989) *J. Biol. Chem. 264*, 13975−13978.
Müller, B., Restle, T., Kühnel, H., & Goody, R. S. (1991a) *J. Biol. Chem. 266*, 14709−14713.
Müller, B., Restle, T., Reinstein, J., & Goody, R. S. (1991b) *Biochemistry 30*, 3709−3715.
Oude-Essink, B. B., Das, A. T., & Berkout, B. (1995) *J. Biol. Chem. 270*, 23867−23874.
Panet, A., & Berliner, H. (1978) *J. Virol. 26*, 214−220.
Panet, A., Haseltine, W. A., Baltimore, D., Peters, G., Harada, F., & Dahlberg, J.E. (1975) *Proc. Natl. Acad. Sci. U.S.A. 72*, 2535−2539.
Press, W. H., Flannery, B. P., Teukolsky, S. A., & Vetterling, W. T. (1989) in *Numerical Recipes in Pascal: the Art of Scientific Computing*, Cambridge University Press, Cambridge.
Richter-Cook, N. J., Howard, K. J., Cirino, N. M., Wöhrl, B. M., & LeGrice, S. F. J. (1992) *J. Biol. Chem. 267*, 15952−15957.
Rigler, R., & Wintermeyer, W. (1983) *Annu. Rev. Biophys. Bioeng. 12*, 475−505.
Rittinger, K., Divita, G., & Goody, R. S. (1995) *Proc. Natl. Acad. Sci. U.S.A. 92*, 8046−8049.
Rodgers, D. W., Gamblin, S. J., Harris, B. A., Ray, S., Culp, J. S., Hellmig, B., Woolf, D. J., Debouck, C., & Harrison, S. C. (1995) *Proc. Natl. Acad. Sci. U.S.A. 92*, 1222−1226.
Rodnina, M. V., Fricke, R., & Wintermeyer, W. (1993) in *The Translational Apparatus: Structure, Function, Regulation, Evolution* (Nierhaus, K. H., Franceschi, F., Subramanian, A. R., Erdmann, V. A., & Wittmann-Liebold, B., Eds.) pp 317−326, Plenum Press, New York.
Saenger, W. (1988) in *Principles of Nucleic Acid Structure* (Cantor, C. R., Ed.) pp 331−349, Springer-Verlag, New York.
Sambrook, J., Fritsch, E. F., & Maniatis, T. (1989) in *Molecular Cloning: A Laboratory Manual* (Irwin, N., Ford, N., Nolan, C., & Ferguson, M., Eds.) pp 10.60−10.61, Cold Spring Harbor Laboratory Press, Cold Spring Harbor, NY.
Sarih-Cottin, L., Bordier, B., Musier-Forsyth, K., Andreola, M., Barr, P. J., & Litvak, S. (1992) *J. Mol. Biol. 226*, 1−6.
Sobol, R. W., Suhadolnik, R. J., Kumar, A., Lee, B. J., Hatfield, D. L., & Wilson, S.H. (1991) *Biochemistry 30*, 10623−10631.
Söll, D. (1993) in *The RNA World* (Gesteland, R. F., & Atkins, J. F., Eds.) pp 157−184, Cold Spring Harbor Laboratory Press, Cold Spring Harbor, NY.
Striker, G., Labuda, D., & Vega-Martin, M. C. (1989) *J. Biomol. Struct., Dyn. 7*, 235−255.
Weiss, S., König, B., Morikawa, Y., & Jones, I. (1992a) *Gene 121*, 203−212.
Weiss, S., König, B., Müller, H. J., Seidel, H., & Goody, R. S. (1992b) *Gene 111*, 183−197.
Wöhrl, B. M., Ehresmann, B., Keith, G., & LeGrice, S. F. J. (1993) *J. Biol. Chem. 268*, 13617−13624.
Wöhrl, B. M., Tantillo, C., Arnold, E., & LeGrice, S. F. J. (1995) *Biochemistry 34*, 5343−5350.

BI9526387